



ECOSYSTEMS

Mobility, bioavailability and distribution of Fe and Cu in mangroves (*Avicennia schaueriana* and *Rhizophora mangle*) from a semiarid coast in NE Brazil

LUIZ D. LACERDA, INGRA B.K. CAVALCANTE, ARLETE A. SOARES & ROZANE V. MARINS

Abstract: Mangroves buffer metals transfer to coastal areas though strong accumulation in sediments making necessary to investigate metals' bioavailability to plants at the rhizosphere. This work evaluates the effect of mangrove root activity, through iron plaque formation, on the mobility of iron and copper its influence on metals' uptake, and translocation through simultaneous histochemical analysis. The Fe^{2+} and Fe^{3+} contents in porewaters ranged from 0.02 to 0.11 μM and 1.0 to 18.3 $\mu\text{g.l}^{-1}$, respectively, whereas Cu concentrations were below the method's detection limit ($<0.1 \mu\text{M}$). In sediments, metal concentrations ranged from 12,800 to 39,500 $\mu\text{g.g}^{-1}$ for total Fe and from 10 to 24 $\mu\text{g.g}^{-1}$ for Cu. In iron plaques, Cu concentrations ranged from 1.0 to 160 $\mu\text{g.g}^{-1}$, and from 19.4 to 316 $\mu\text{g.g}^{-1}$ in roots. Fe concentrations were between 605 to 36,000 $\mu\text{g.g}^{-1}$ in the iron plaques and from 2,100 to 62,400 $\mu\text{g.g}^{-1}$ in roots. Histochemical characterization showed Fe^{3+} predominance at the tip of roots and Fe^{2+} in more internal tissues. *A. schaueriana* showed significant amounts of Fe in pneumatophores and evident translocation of this metal to leaves and excretion through salt glands. Iron plaques formation was essential to the Fe and Cu regulation and translocation in tissues of mangrove plants.

Key words: Bioavailability, iron plaque, metals, porewater, rhizosphere, sediment.

INTRODUCTION

Waterlogged soils submit plants to suboxic or anoxic conditions at the rhizosphere level that can lead to the accumulation of reduced forms of toxic substances. As a response, plants transfer and exude oxygen at the root level (Radial Oxygen Loss - ROL), oxidizing chemical species and decreasing their toxicity to the plant (Pi et al. 2011, Cheng et al. 2010, 2020, Nath et al. 2013). The development of extensive aerenchyma tissue in the roots facilitates ROL by reducing the diffusive resistance to the longitudinal transport of gases from the aerial parts to the roots and decreasing the oxygen demand per unit of volume, naturally promoting a greater

supply of oxygen to the apical ends of the roots (Colmer 2003). ROL induces precipitation of iron as Fe^{3+} -oxides, forming iron plaques covering the surface of roots that act as a barrier by immobilizing toxic metals dissolved in porewaters and reducing their uptake by plants. ROL increases plant tolerance to flooding and to changes in physical-chemical parameters (pH, Eh, dissolved oxygen) of soils and porewaters, affecting nutrients and trace metals availability (Hu et al. 2007, Cheng et al. 2015, Pi et al. 2011).

Mangroves are considered sources and/or sinks of chalcophiles trace metals that precipitate and accumulate in sediments as sulfides, a product of the sulfate reduction

metabolism typical of these ecosystems. At the root level, however, oxidation of sulfides by ROL may dissociate metal sulfides and release metals to porewaters that can either be re-precipitated on iron plaques or complexed with dissolved organic compounds and eventually exported to adjacent waters (Lacerda et al. 2022). On the other hand, ROL also induces the formation of poorly crystalline iron minerals, that at least in part, may enhance metal bioavailability (Araújo et al. 2016).

The definitive role of mangroves as sink or source of metals will depend on the site-specific physical chemical characteristics and of the different mangrove species colonizing the site, since different mangrove species promotes different changes in sediment and porewater chemistry (Lacerda et al. 1993). The genera *Rhizophora* and *Avicennia* are the most widely distributed mangroves worldwide. In Brazil, *R. mangle* and *A. schaueriana* are the most dominant species along the entire mangrove distribution. Both develop highly dense and

complex root systems and have shown to strongly affect soil biogeochemistry (Lacerda et al. 1993, 2022).

This work aims to evaluate the effect of the mangrove root activity and the presence of iron plaques on the biogeochemistry and bioavailability of Fe and Cu and their distribution in roots and leaves of the species *R. mangle* and *A. schaueriana*, the dominant mangrove trees in the northeastern Brazil, in the Jaguaribe river estuary, the largest mangrove area among river estuaries draining at the semiarid coast, and where metal emissions are on the rise due to anthropogenic sources.

MATERIALS AND METHODS

Study area and sampling

The studied mangrove in the Jaguaribe river estuary ($4^{\circ} 26' S$ and $37^{\circ} 47' W$) (Figure 1) is under a hot semiarid climate, with average annual rainfall of 764 mm, occurring mostly from January to May, and temperatures varying

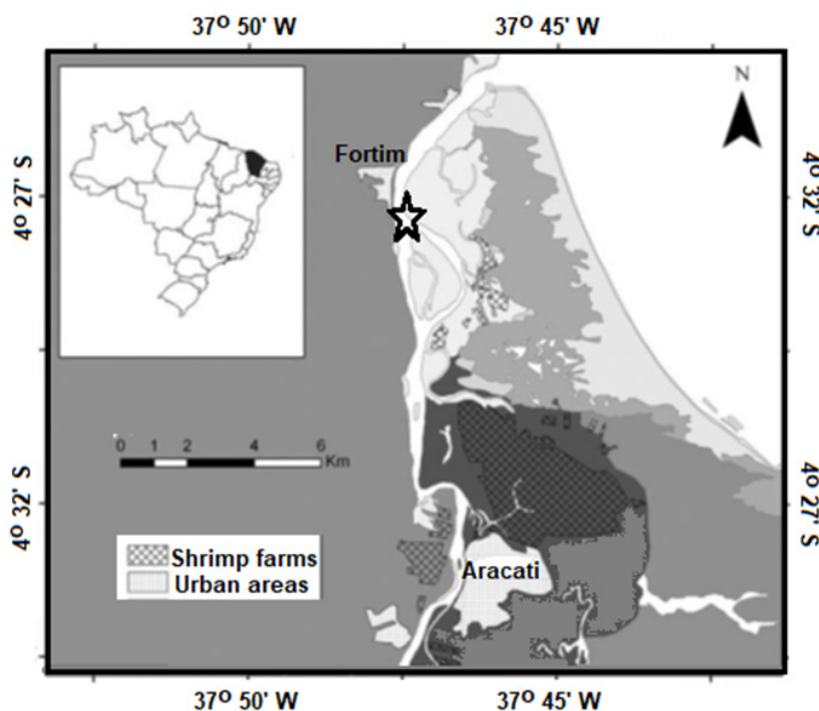


Figure 1. Thematic map and location map of the Jaguaribe River estuary, NE Brazil, with a focus on urban areas and larger shrimp farming areas, mangrove sampling site is marked by a star.

between 26°C and 28°C. During the study period (2016-2017) an extreme drought period lowered annual rainfall to 506 mm compared to the historical mean of 794 mm (FUNCEME 2022). The estuary has a length of 36 km, is under a semidiurnal tidal regime with highest amplitude of 2.8 m and occupies an area of approximately 3,050 km² with total water flux varying from 22 to 57 m³.s⁻¹ (Dias et al. 2018). Major drivers of metal contamination to the estuary are intensive shrimp aquaculture, covering about 3,040 ha in the middle and upper estuary, responsible by c.a. 12% of the national shrimp production, where the chronic use of Cu-bearing aquafeeds and fertilizers causes anomalous Cu contents in water and sediments of adjacent mangroves (Lacerda et al. 2006). Two medium size cities (Aracati and Fortim) and several small villages, totaling about 100,00 inhabitants, with only partial treatment of wastewaters and urban solid wastes (Marins et al. 2020) (Figure 1), also contribute to Cu emissions. The studied site is a fringe mangrove forest composed by *Rhizophora mangle* and *Avicennia schaueriana*, and sparsely distributed shrubs of *Laguncularia racemosa*. The three species are mixed and show no zonation in the studied forest. The taxonomic identification of the mangrove plants was done through morphological characteristics of the root system and leaf anatomy following Tomlinson (1986).

At the sampling station, two sediment cores (S1 and S2 about 10 m apart) were collected using acrylic tubes of 4.0 and 5.7 cm in diameter to a depth of 60 cm, which includes the layer of maximum root biomass as observed in most mangroves (Ong Che 1999, Chakraborty et al. 2015) and guarantee the recovery of the first 50 cm of sediments usually proposed by Blue Carbon Protocols and therefore, being globally comparable (Howard et al. 2014). Two additional acrylic tubes were used for quantitatively

collecting roots of *R. mangle* and *A. schaueriana* for analysis. Leaves from 10 trees of each species were also sampled. All sediment sampling and measurements were performed in duplicate. Five porewater collectors consisted of a PVC tube with a ceramic cap attached, with approximate pore size of 0.7 mm, were inserted at depths of 0 cm, 10 cm, 15 cm, 30 cm, 40 cm and 50 cm in the sediment. Vacuum was created by hand pumps and the tubes left for 5 hours. Vacuum was verified and corrected every 1 h. After, porewaters were extracted directly from the tubes with syringes and Nalgene® flexible tubes and immediately frozen in ice, thus avoiding significant changes in porewater physical-chemical characteristics (Supplementary Material Figure S1).

Porewaters and sediment treatment and analysis

Temperature, pH and Eh were obtained directly from the collection tubes with the aid of a portable pH meter (Hanna Instruments, model HI98121) to avoid contact of the sample with the atmosphere and not compromise the samples for the analysis of Fe speciation in porewaters due to oxygenation. Quantification of Fe fractions (dissolved Fe²⁺ and particulate Fe³⁺) in porewaters followed Viollier et al. (2000). For Fe²⁺ quantification, 100 to 200 ml of Ferrozine (acid monosodium salt hydrate of 3 - (2-pyridyl) -5,6-diphenyl-1,2,4-triazine-p, p'-disulfonic acid) were added in the vials immediately after collection in the proportion of 10% of the sample volume, the stable magenta complex formed were spectrophotometric quantified at wavelength 562 nm, at pH between 4.0 and 9.0. Subsequently, a reducing agent (1,4M hydroxylamine hydrochloride) and a buffer (30% ammonium hydroxide) were added to determine the total Fe in the sample. Samples were stored in amber bottles and analyzed immediately after arrival at the laboratory. All materials that

came into contact with the samples were pre-washed with acid (1 N HCl) and left from 24 h in a Extran® bath solution. The detection limit of the method was 0.2 μM . The concentrations of Cu in porewaters, however, could not be detected by the atomic spectrophotometric method used and were always below the detection limit (<0.1 μM).

Sediment cores were sectioned in samples of 1 cm thickness (Figure S1), each sample was analyzed for grain size, by sieving and weighing fractions, total organic carbon (TOC), iron (Fe) and copper (Cu) concentrations. Sediments TOC contents were quantified by adding 5.0 mL of $\text{K}_2\text{Cr}_2\text{O}_7$ (0.167 mol L^{-1} solution) and 10 mL of concentrated H_2SO_4 to 0.1 g dried sediment in 100 ml glass vials. Vials were taken to a preheated digester block at 170 °C for 30 min. After colling extracts were transferred to an Erlenmeyer titrated with $\text{Fe}(\text{NH}_4)_2(\text{SO}_4)_2 \cdot 6\text{H}_2\text{O}$ 0.2 mol. L^{-1} (Mohr Salt) (Yeomans & Bremner 1988).

Sub-samples were oven-dried at 50°C to constant weight, sieved and macerated. Approximately 0.3 g of dried samples were digested with 10 ml of a 50% aqua-regia solution ($4\text{H}_2\text{O}:3\text{HCl}:1\text{HNO}_3$) in a Mars Xpress (CEM Corporation) microwave digester. Quantification of Fe and Cu was performed by Atomic Absorption Spectrophotometry (AAS), in AA-6200 Shimadzu spectrophotometer using 1,000 $\mu\text{g L}^{-1}$ standard solutions (Merck®). Reference standard, NIST 1646A estuarine sediment was simultaneously analyzed for precision of the methods.

The limit of detection (LD) is the smallest analyte mass possible to be quantified and statistically different from the method's blanks at a confidence level of 99%. The calculated LD (based on a Student's t-distribution) for sample blanks (n = 7) is multiplied by the factor of 3.14 (USEPA 2000). When blank absorbances were lower than the detection limit of the equipment, LD was calculated using Excel 2010 function

“EpadYX” of the different metal concentration and absorbance. As such, for sediments, Fe mean LD was $4.04 \pm 0.01 \mu\text{g.g}^{-1}$, and the mean reference standard recovery was $88 \pm 11 \%$. Cu mean LD was $0.2 \pm 0.1 \mu\text{g.g}^{-1}$ and the mean reference standard recovery was $89 \pm 7 \%$.

Plants treatment and analysis

Cores used for roots sampling were immediately frozen and then transported to the laboratory, after extraction from the mangrove soil. When thawed, roots were washed twice with reverse osmosis distilled water to remove sediment particles adhered to root surfaces. After washing, roots were freeze dried for 4 days and stored in previously acid-washed (1N HCl) glass jars until analysis, for biomass quantification and total Fe and Cu concentrations.

Completely expanded leaves (n = 20 each) were collected from healthy adult individuals of *R. mangle* and *A. schaueriana* for the histochemical analyses of Fe distribution in leaves and roots. Leaves were cut with a stainless-steel blade carefully avoiding embolism of the conducting vessels. Roots were collected from juvenile individuals (35-40 cm height). The collected material was stored in plastic bags inside Styrofoam with ice and sent to the plant anatomy laboratory and preparation for analysis within 24 hours.

All samples were previously washed with distilled water to remove any particles deposited on the surface. Then the fresh plant material was cross sectioned by hand and separated into two parts for determinations of Fe^{2+} and Fe^{3+} . The first part of the sectioned material was inserted in Perl reagent, solution composed of potassium ferrocyanide 1% ($\text{K}_3\text{Fe}(\text{CN})_6$) and HCl 2% in the ratio 1:1 for determination of Fe^{3+} . The other part of the sectioned tissues was immersed in Lillie's reagent, composed of 400 mg of potassium ferrocyanide dissolved in 40 ml of 5% HCl

(Bancroft et al. 2008) for detection of Fe^{2+} . After 24 hours, the “cuts” were washed with distilled water and the photographs were analyzed with the aid of an optical microscope (LEICA DM400) coupled with an image capture system. The positive staining was verified by the Prussian blue color of the Perl reagent (ferric iron), or by the Turnbull blue of the Lillie’s reagent (ferrous iron).

For the extraction of iron plaques, the samples were weighed in an Erlenmeyer and stirred for 3 hours in a solution of Dithionite-Citrate-Bicarbonate (DCB) (40 mL of 0.3 M sodium citrate ($\text{Na}_3\text{C}_6\text{H}_5\text{O}_7\cdot 2\text{H}_2\text{O}$), plus 5 mL of 0.1 M sodium bicarbonate (NaHCO_3) and 3 g of sodium dithionite ($\text{Na}_2\text{S}_2\text{O}_4$) at 25° C (Taylor & Crowder 1983). After extraction, the solution was filtered in a Millipore filtration kit (Merck) coupled to a suction pump, for root separation. Then, the roots were washed three times, using 15 ml of distilled water for each wash. The solutions generated from the washes were separated and diluted to the volume of 100 ml with Milli-Q® to the quantification of metals, immediately after extraction and using AAS.

Root previously washed in DCB solution were dried in an oven at 37°C for 72 hours or until they were completely dry and homogenized with mortar and pestle for digestion. Total digestion of these samples used a 50% *aqua-regia* solution (HNO_3 , HCl and H_2O ; 1:3:1). The digestion was performed in a microwave oven digester (MARS XPRESS, CEM Corporation) at 200°C for 30 minutes; after, 1 mL of H_2O_2 was added and the final extract transferred quantitatively with MilliQ® water to 100 mL in volumetric flasks. All glassware and materials used were previously washed in a neutral detergent bath followed by immersion for 24 hours in a Hg-free HCl 10% solution. Quantification was also performed by atomic absorption spectrophotometer. The use of this acid composition for the extraction

of metals from plant tissues was previously used by Marchand et al. (2006), but in different concentrations.

Certified reference standards, dried leaves of aquatic plant *Lagarosiphon major* (BCR 060), were simultaneously analyzed to determine the accuracy and recovery of the method. Mean recovery was $84 \pm 7\%$ for Fe and $94 \pm 6\%$ for Cu. Detection limits, calculated for sediment samples were $6.5 \mu\text{g.g}^{-1}$ for Fe and $0.2 \mu\text{g.g}^{-1}$ for Cu. The concentration values were not corrected for the relative recoveries obtained for the certified material.

Statistical analysis

Despite considering a single sampling point, data from each profile was analyzed separately, since both sediment and root profiles presented different distribution patterns. Since the data obtained did not meet the normality requirements verified by the Shapiro-Wilk test, for each profile collected, correlations used Spearman’s r . Comparisons between sediment and root metal concentrations used non-parametric Wilcoxon test. The significance value was 95% ($p < 0.05$). Statistical tests and graphs used R Studio version 1.1.442 (RStudio Inc 2009-2018) and Microsoft Office 2010 (©Microsoft Corporation 2010).

RESULTS AND DISCUSSION

Root biomass, temperature, pH, Eh and iron in pore waters

Root biomass, temperature, pH, Eh, Fe^{2+} and Fe^{3+} in interstitial water are shown in Table I, relative to sediment core depth. Range of root biomass (Figure 2) integrated for 10 cm layers and from the two cores, showed highest root biomass below the 30 cm layer downward to the core base and varied from 2.5 to 3.9 g per 10 cm-layer, compared to the first 30 cm with

Table I. Root biomass (integrated for 10 cm layers), temperature, pH, Eh, Fe²⁺ and Fe³⁺ in interstitial water in the studied mangrove fringe forest in the Jaguaribe River estuary, NE, Brazil.

Depth (cm)	Root biomass (g)	Temperature (°C)	pH	Eh (mV)	Fe ²⁺ (µM)	Fe ³⁺ (µM)
0-2	-	31.1	5.78	-60	10	75
2-10	1.7-2.5	31.3	5.98	-133	35	330
10-20	1.6-1.8	31.7	6.86	-88	15	250
20-30	1.5-2.3	31.4	7.19	-89	<0.2	20
30-40	3.8-3.9	31.4	6.85	-76	5	120
40-50	2.6-2.5	31.1	7.08	-73	<0.2	45

biomass varying from 1.6 to 2.3 g per 10 cm-layer. Temperature did not vary with depth and the observed range of values is optimal to the proper physiological conditions of roots; pH was slightly acidic (5.78 – 5.98) at the more surface layers to 10 cm, and neutral at greater depths (6.86 – 7.19), whereas Eh characterizes sediments as mild to moderately reducing and together with the observed pH range favor the formation of iron plaques around mangrove roots (Xu & Yu 2013). While blocking of oxygen intrusion into the sediment strongly increases iron plaque formation directly influencing the translocation and regulation of metals and nutrients by plants, slightly acidic to circum-neutral pH do not provide excess H⁺ ions that could prevent the formation of iron plaques (Batty et al. 2000).

There is a clear relationship between root biomass and Eh, maximum root biomass corresponds to less reducing Eh (10 to 30 cm), suggesting ROL from roots to affect redox conditions, as shown for other wetland sites (Lacerda et al. 1993, Marins et al. 1997, Otero et al. 2006, Tripathi et al. 2014). Mangrove porewater were enriched in Fe²⁺ and Fe³⁺, but concentrations vary significantly with depth. Both fractions show highest concentrations in the top 15 cm; Fe²⁺ reaches a maximum of 35 µM at 10 cm depth, whereas Fe³⁺ also peaked at 10 cm, but with

much higher concentrations (330 µM). Below 30 cm of depth Fe²⁺ nearly disappeared, suggesting upward migration as dissolved species, whereas Fe³⁺ concentrations are lower, but still significant even in the deepest layer. This significant decreases in Fe²⁺ concentrations may also be associated with higher sulfide contents in the pore water favoring iron precipitation as pyrite (Otero et al. 2006).

The presence of reducing conditions that facilitate the reactive dissolution of precipitate iron compounds and produce Fe²⁺ along with ROL are more important factors than the amount of Fe present in the environment. The establishment of plants induce changes in interstitial water chemistry, such as decreased sulfide concentrations and changes in redox potential, but the extent of these changes is different for each species, and differences can also be observed at the individual level (Otero et al. 2006, Inque et al. 2011, Tripathi et al. 2014). Notwithstanding, the range of Fe²⁺ concentrations found in mangrove porewaters from the Jaguaribe Estuary compares to those reported for other mangroves worldwide. Concentrations from four mangrove sites in Australia varied from a highest value in Moreton Bay (347 µM), to a lowest at Hinchinbrook (0.54 µM) and intermediate at Darwin (17.4 µM) and

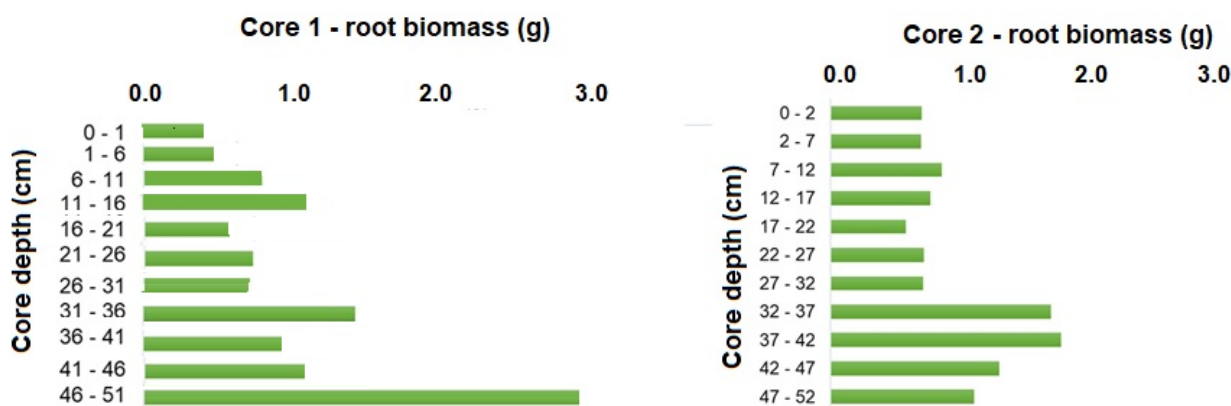


Figure 2. Root biomass distribution in sediment cores from fringe mangroves at the Jaguaribe River Estuary, NE, Brazil.

Seventeen Seventy ($42.4 \mu\text{M}$) (Holloway et al. 2016). In southeastern Brazil, Kristensen et al. (2023) showed solid phase reactive iron (Fe^{3+}) and Fe^{2+} also decreasing with sediment depth and with Fe^{2+} concentrations varying from ~ 0 to $140 \mu\text{M}$. Dissolved iron (Fe^{2+} and Fe^{3+}), also determined by colorimetric procedure like in this present study, in porewaters from New Caledonian *Avicennia* and *Rhizophora* mangrove stands, showed maximum concentrations of both forms in the upper 20 cm, of up to $100 \mu\text{M}$, and decreased with depth. In the upper oxic layers, however, there is an absence of Fe^{3+} and very low concentrations of Fe^{2+} that may indicate that iron oxide reduction did not occur in these upper sediment layers or that as soon as it is produced, Fe^{3+} precipitates as ferrihydrite and lepidocrocite (Deborde et al. 2015).

Grain size, organic carbon and metal concentrations in sediments

Grain size in both cores was predominantly of fine sands, with low fractions of gravel and of silt/clay grain sizes. Profile S1 and S2 showed fine sand content from 89 to 96% and silt/clay fraction from 1 to 8%. In the first 9 cm of depth, the percentage of fine material was always less than 1%, whereas below this depth the silt/clay fraction was higher and varied 3% to 13%. The

low proportion of silt/clay sediments are typical of the Jaguaribe estuary where large transport of sands from adjacent dune fields reaches the local mangroves (Jimenez et al. 1999) but is lower than typical mangrove sediments reported elsewhere (Souza et al. 2016).

Total organic carbon (TOC) and *aqua regia* extracted Cu and Fe concentrations presented a similar distribution in the two cores. Average values relative to sediment depth are presented in Figure 3. Average TOC contents decreased steadily with depth from 3.1 % at the surface to 1.3% at 25 cm depth, increasing to 2.1% in the deepest layers. The TOC distribution seems to reflect the distribution of root biomass, which also presented maximum values below 30 cm of depth. The higher values at the surface of the sediment may reflect recent deposited abundant litter typical of mangroves. *Aqua regia* extracted Cu concentrations were relatively constant in both cores but with slightly decreasing concentrations with depth from $19.8 \mu\text{g.g}^{-1}$ in the surface layers and reaching a minimum, at 12 cm, of $14.8 \mu\text{g.g}^{-1}$. From 30 cm of depth Cu to the core bottom concentrations increased again to similar values of those at the surface ($\sim 20 \mu\text{g.g}^{-1}$). These Cu concentrations, but not those of Fe, are much lower than those

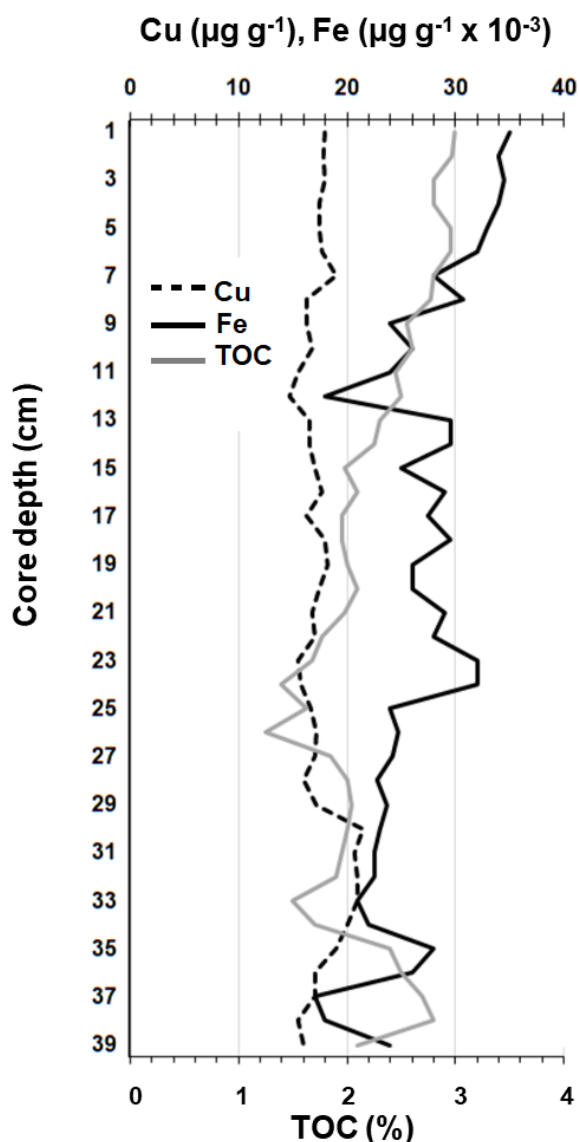


Figure 3. Total organic carbon (TOC), and *aqua regia* extracted Cu and Fe concentrations relative to mangrove sediment depth from the Jaguaribe estuary, NE Brazil. Average of the two cores.

observed in contaminated mangroves (Kumar & Ramanathan 2015, Machado et al. 2005). Average Fe concentrations were more variable, but also decreasing from high values at the surface ($34,500 \pm 8 \mu\text{g.g}^{-1}$) to a minimum at 12 cm of depth ($18,000 \mu\text{g.g}^{-1}$). Increasing again to the observed values in surface layers to about 30 cm and showing higher concentrations in the deepest layers (up to $31,000 \mu\text{g.g}^{-1}$).

The near “S”- shaped curve observed for Cu and Fe seems to reflect redox conditions observed in porewaters, with less reducing conditions at the 10 cm surface layers increasing to a peak subtoxic conditions at around 10 cm ($E_h = -133$), to intermediate values to 30 cm and less reducing conditions below, covarying with root biomass increase. This shifting redox conditions due to more aerobic conditions at the surface and at the root zone of the sediments, to strong anaerobic conditions has been reported to control trace metal distribution in mangrove sediments, particularly chalcophile elements (Alongi et al. 2004, Otero et al. 2006, Pi et al. 2011, Nath et al. 2013).

Concentrations of Cu and Fe in roots, iron plaques and leaves

Concentrations Cu and Fe in roots and iron plaques sampled from cores were quite variable depending on soil depth in the two cores (Figure 4). The concentrations of Cu associated with iron plaques in core 1 ranged from a minimum of $1.5 \pm 0.5 \mu\text{g.g}^{-1}$ (at 50 - 60 cm), reaching a maximum of $81.7 \mu\text{g.g}^{-1}$ in the first 10 cm of the soil. Whereas in core 2, they ranged from $29.6 \pm 0.04 \mu\text{g.g}^{-1}$ (at 30 - 40 cm) to $161.1 \mu\text{g.g}^{-1}$ (at 15 - 25 cm). Copper concentrations in the residual root material, the proportion actually incorporated by roots, in core 1, ranged from a minimum of $19.4 \pm 3.9 \mu\text{g.g}^{-1}$ at a depth of 66 - 71 cm to a maximum of $316 \pm 39.5 \mu\text{g.g}^{-1}$ at a depth of 86 - 91 cm. Whereas in core 2, Cu concentrations in the residual root material ranged from $22.1 \pm 14.1 \mu\text{g.g}^{-1}$ at a depth of 32 - 37 cm to a concentration of $295.0 \mu\text{g.g}^{-1}$ at a depth of 17 - 22 cm.

Iron plaques contribute to an average fraction of the total Cu content in roots varying from 25.8 % to 42.7 %, depending on core and sample depth. Minimum contribution occurred in less reducing E_h , whereas maximum

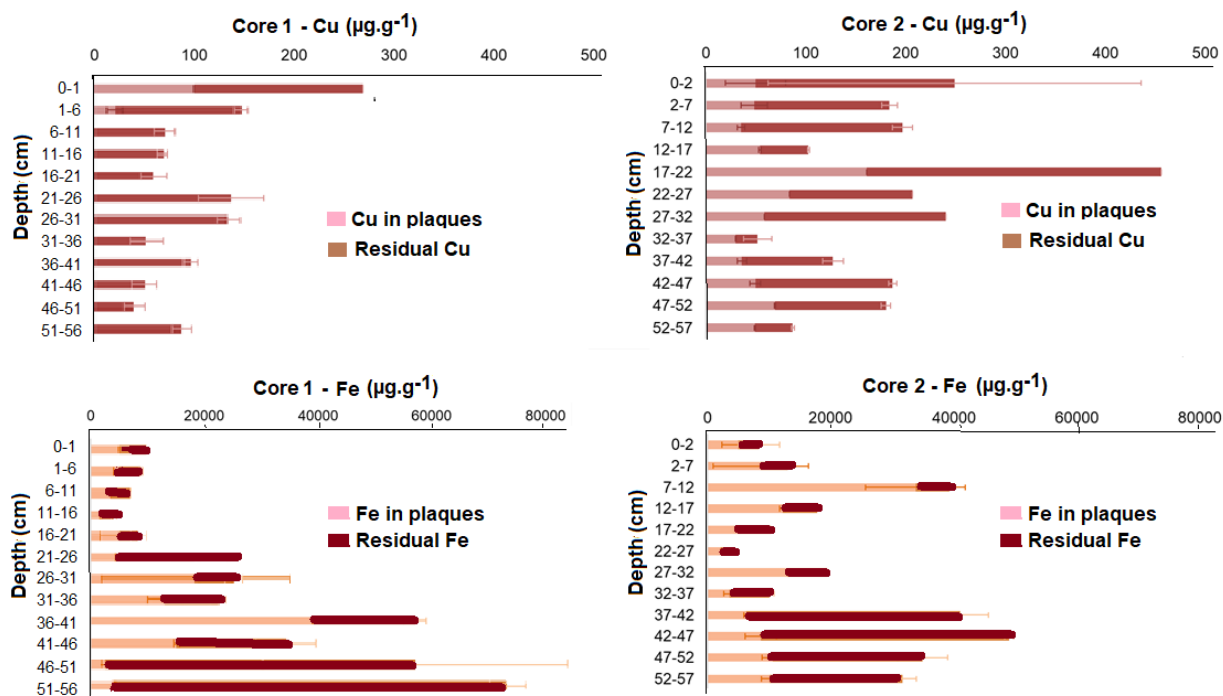


Figure 4. Vertical distribution of Cu and Fe in roots and iron plaques from mangrove sediment cores at the Jaguaribe river Estuary, NE, Brazil.

contribution occurred in the more reducing conditions.

The concentrations of Fe associated with iron plaques in core 1 ranged from a minimum of $606 \pm 93 \mu\text{g.g}^{-1}$, at 76 - 81 cm, to a maximum of $36,000 \pm 190 \mu\text{g.g}^{-1}$, at 36 - 41 cm. Whereas in core 2, Fe concentrations associated with plaques ranged from $2,084 \mu\text{g.g}^{-1}$ at 22 - 27 cm and $33,819 \pm 8,102 \mu\text{g.g}^{-1}$ at 7 - 12 cm. Iron concentrations in the residual root material, the proportion actually incorporated by roots, in core 1, varied from $2,100 \pm 513 \mu\text{g.g}^{-1}$, at 11 - 16 cm depth, to $62,440 \pm 2,870 \mu\text{g.g}^{-1}$, at a depth of 51-56 cm. Whereas in core 2, Fe concentrations in the residual root material varied from $2,442 \mu\text{g.g}^{-1}$, at a depth of 22 - 27 cm to $40,323 \pm 718 \mu\text{g.g}^{-1}$, at 42 - 47 cm depth. Iron plaques contribute to 35% to 40% of the total Fe content in the first 50 cm of the sediment, below this depth, the iron plaques contribute with about 10% to 20% of the total Fe content.

Most iron, particularly below 50 cm of depth, is incorporated into the root tissues proper.

The average concentration of Cu in *R. mangle* leaves was $14 \pm 1.1 \mu\text{g.g}^{-1}$, while of Fe it was $135.8 \pm 10.5 \mu\text{g.g}^{-1}$. Leaves of *A. schaueriana* showed average concentrations of Cu ($17 \pm 1.5 \mu\text{g.g}^{-1}$), similar to *R. mangle* leaves, while Fe concentrations were three times higher than those measured in *R. mangle* ($346.5 \pm 40.2 \mu\text{g.g}^{-1}$). Concentrations of Cu are 10 times higher than those reported for these species in mangroves from southern Brazil, where soil redox potential are extremely negative (-316 to -327) (Madi et al. 2015), suggesting that the less reducing conditions of the semiarid mangroves of the Jaguaribe estuary results in higher metals availability to plant uptake. Although mangroves accumulate metals from the sediments, low concentrations are generally found in the leaves of mangrove plants (MacFarlane et al. 2007). The ability to accumulate metals, the physiological responses

to them, and the ecological risks associated with these contaminants to mangroves have been studied by several authors, as well as their association with iron plates, radial oxygen loss, and tolerance to flooding (Chaudhuri et al. 2014, Cheng et al. 2015, Naidoo et al. 2014), as well as on the mangrove's role in the transfer of metals to estuarine and coastal environments (Alongi et al. 2004, Arrivabene et al. 2015, 2016, Cheng et al. 2010, 2015, Liu et al. 2009, MacFarlane et al. 2007).

Differences between metal concentrations between these two pantropical genera of mangroves have been reported in many regions. Alongi et al. (2004) evaluating concentrations of Fe and Cu in *R. stylosa* and *A. marina* on the west coast of Australia, found Fe contents in leaves of these species varying from 127 to 360 $\mu\text{g}\cdot\text{g}^{-1}$ and 137 to 859 $\mu\text{g}\cdot\text{g}^{-1}$, respectively, whereas Cu concentrations varied from 3.4-4.1 $\mu\text{g}\cdot\text{g}^{-1}$ in leaves of *R. stylosa* and from 6.5 to 8.6 $\mu\text{g}\cdot\text{g}^{-1}$ in *A. marina*. Bernini et al. (2006) also found higher concentrations of Fe in leaves of *A. schaueriana* than in *R. mangle*, in SE Brazil. These differences were associated with different physiological adaptations to high soil salinity, namely "salt exclusion" in *Rhizophora* and "salt translocation and excretion" in *Avicennia* (Machado et al. 2005). In addition, by comparing living and dead roots, Alongi et al. (2004) suggested that most of the Fe in the plant was associated with living fine roots, both in *Rhizophora* and in *Avicennia*. These results agree with our findings. Abou Seedo et al. (2017) studying metals concentrations in sediments and leaves of mangroves from different sites in Bahrain suggested that mangrove leaves respond to concentrations of bioavailable Cu in the environment. On the other hand, Chakraborty et al. (2015) concluded that Cu accumulation in mangrove roots did not gradually increase with increasing total Cu load and Cu association with organic phases in

sediments. Since our results are from a single site along the estuary, there is no possibility of checking any response of mangrove plant metal contents to different metals loads to the environment. In the present work it was not possible to perform sequential extractions to evaluate the behavior of Cu in relation to the fractions bound to organic matter. However, no positive relationship was found between copper and biomass contents. Histochemical tests on living fine roots, that will be presented further however, may help understand the relationship between sediment and plant metal concentrations.

Histochemistry of Fe in roots and leaves of *A. schaueriana*

The root epidermis of *A. schaueriana* was the main site of Fe bioaccumulation, showing a positive reaction to the histochemical tests for both Fe^{2+} and Fe^{3+} . The accumulation of metals in mangroves occurs mainly in the root zone and together with the formation of iron plates results in a limited translocation of these metals to the aerial parts of the plant, such as the trunk, leaves and flowers (MacFarlane et al. 2000, 2003, Machado et al. 2005).

In the thin roots of *A. schaueriana* where a small and weak coloration is observed (Figure 5a, b), indicating little presence of Fe^{2+} associated with the root epidermis. However, for Fe^{3+} , the positive reaction was quite intense showing Prussian blue color positive around the entire epidermis of the root (Figure 5d, e). The stronger positive reaction indicates the presence of precipitated iron mainly around the root. This result indicates the functioning of the epidermis as the first barrier to Fe absorption by mangrove plants (Arrivabene et al. 2016, Cheng et al. 2015, 2020). Thicker roots presented the same pattern of Fe^{2+} and Fe^{3+} distribution. But a scattered presence of Fe^{2+} can also be observed

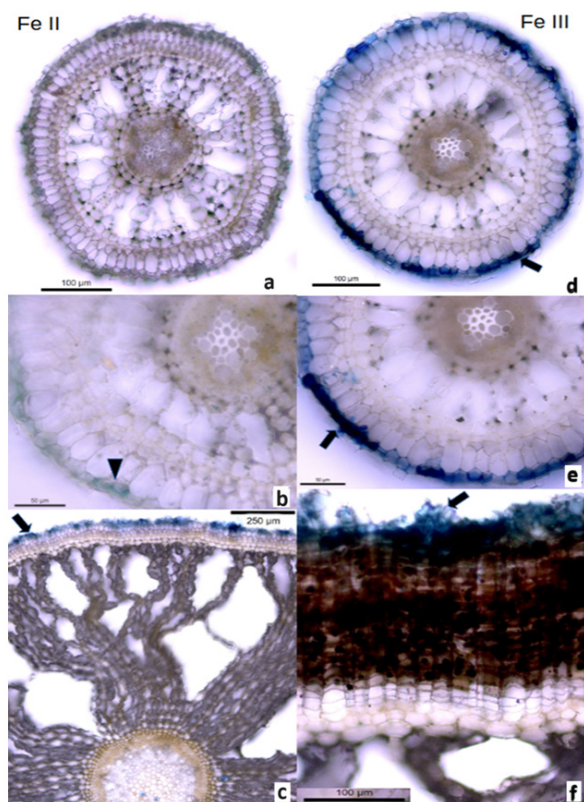


Figure 5. Iron histochemistry in cross-sections of *A. schaueriana* roots. a-c: Fe^{2+} (Fe II) Lillie's reagent. a-b: thin roots and c thick roots. d-f: and Fe^{3+} (Fe III) Perl reagent test. Blue coloration indicates positive reaction to the test.

in the pith region (Figure 5c), whereas Fe^{3+} is exclusively present in the outermost layer of the suber (Figure 5d).

Species of the genus *Avicennia* have complex root systems, with different types of roots (Purnobasuki & Suzuki 2005). The presence of aerial roots mainly, establishes the formation of paths between the atmosphere and the sediments that allows the exchange of gases (Lacerda et al. 1993, Marchand et al. 2011). In Figure 5c-d it is possible to observe the development of aerenchyma, but there was no investigation as to the possible relationship between the development of aerenchyma and the presence of iron plates in the roots. Although Pi et al. (2011) suggested the existence

of an association between the development of aerenchyma in mangrove plants submitted to the effects of effluents disposal and the increase of iron plaques formation due to a greater of radial oxygen loss, our results showed iron mainly on epidermis and outermost layer of the suber. The epidermis is considered the main compartment of Fe bioaccumulation in roots and possibly the most significant barrier to metals absorption by plants (Arrivabene et al. 2016). Metal accumulation may also occur in the endoderm of roots with an apoplastic barrier to metal uptake provided by the Caspari's striae (Di Toppi et al. 2012). In our plant samples however, it was not possible to observe Fe accumulation, both $\text{Fe}(\text{II})$ and $\text{Fe}(\text{III})$, in the Casparian strip or phellogen neither for this species, only in the epidermis corroborating the results from Arrivabene et al. (2016).

In the cross-sections of *A. schaueriana* leaves there is no accumulation of the Fe^{3+} on the mesophyll (Figure 6a, b), but it was positive in the epidermal salt glands (Figure 6c). The presence of Fe^{3+} in the leaves, however, was practically nonexistent in the analyzed sections under the chemical treatment used to detect this chemical form. In a different way, cross-sections of *A. schaueriana* leaves showed Fe^{2+} accumulation in a salt gland, the midrib (Figure 6c), and a strong positive reaction in the hypodermis (Figure 6a), and in the spongy and palisade parenchyma (Figure 6d). This result agrees with the analytical quantification of total Fe in leaves of *A. schaueriana*.

The excretion capacity of toxic solutes is a characteristic mechanism of detoxification of *Avicennia* that have salt secretory glands on the surface of their leaves accumulating metals within these structures that is favored by the ability to transport a large amount of salt within the xylem (Tomlinson 1986, Sruthi et al. 2016, Scholander 1968). Figure 6d shows the presence

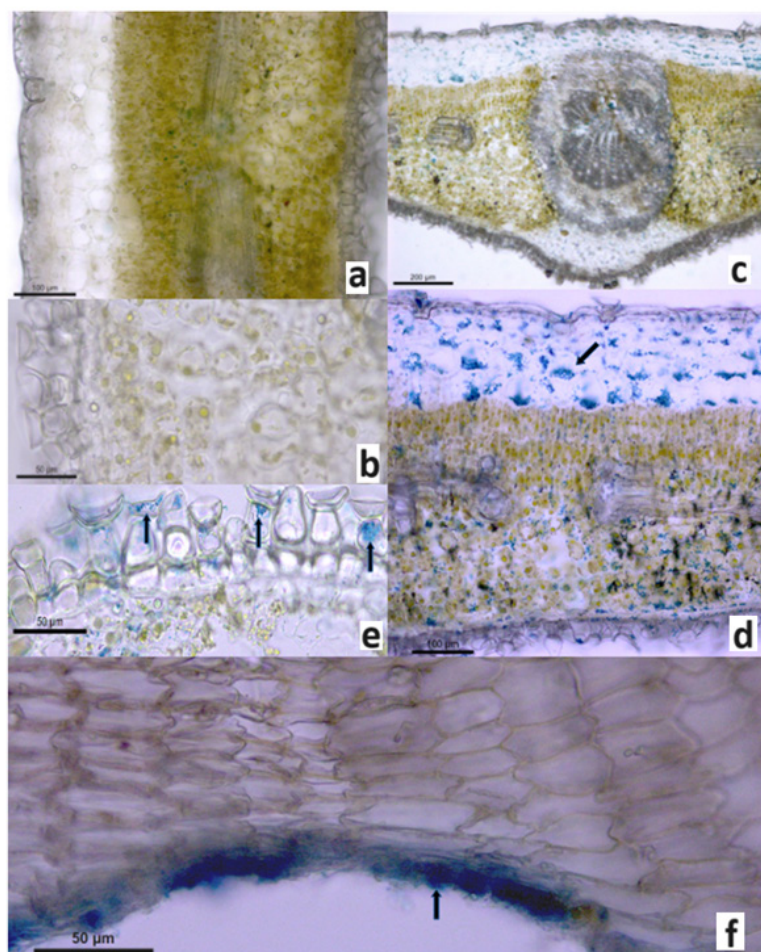


Figure 6. Iron histochemistry in cross-sections of leaves of *A. schaueriana*. a-e. a-b negative Perl reagent for Fe^{3+} . c-e: Lillie's reagent test showing accumulation of Fe^{2+} in the midrib (6c), mesophyll of leaves (6d) and in the salt glands on epidermis (6e). Cross-sections of pneumatophores. f: Fe^{3+} in the outer layer of suber (6f). Blue coloration indicates positive reaction to the test (arrows).

of Fe^{2+} within the secreting glands. Previous studies showed the highest concentrations of Fe in leaves of species that contain salt glands, compared to species that do not have these structures, such as *R. mangle* (Bernini et al. 2006, Cuzzuol & Fields 2001, Souza et al. 2014, 2015), but most did not show the actual presence of metals in the salt excreting glands proper.

There were positive reactions to Fe^{3+} in the outermost layer of the suber of pneumatophores (Figure 6f), indicating that the periderm of pneumatophores is an effective barrier to both dissolved and particulate Fe.

According to Lewis et al. (2011), both thin roots and pneumatophores have been observed to present greater absorption of metals, when compared to leaf tissues, and can be

used together with the roots for monitoring purposes. The analytical quantification of Fe and Cu in pneumatophores was not performed in the present study. However, Nath et al. (2013) comparing concentrations of metals in leaves and pneumatophores of *A. marina*, found that the absorption and accumulation of Fe, Ni and Mn occurs mainly in pneumatophores, while for other metals (Cu, Pb and Zn) accumulation occurs more strongly in the leaves. On the other hand, Souza et al. (2015) suggested that *A. schaueriana* seems to enhance the translocation of metals, including Cu and Fe, to diminish their concentrations in roots. The Fe-secretion through salt gland observed in *A. schaueriana* leaves is one pathway to excretion and diminish

the high concentration of the Fe inside the body of plants.

The quantification of Fe in the leaves may have been efficient due to the amount of Fe present in the tissues, however, it is necessary to analyze a larger number of individuals to obtain more robust data on the behavior of each species in relation to the presence of metals. It would also be interesting to better evaluate the behavior of pneumatophores in relation to the geochemistry of metals at the site.

Histochemistry of Fe in roots and leaves of *R. mangle*

The roots of *R. mangle* showed positive reactions of little intensity or no reaction to the

chemical treatment, especially for Fe²⁺ (Figure 7a-d). In the images of Figure 7b, it is possible to notice the thick exoderm of the root even in thin roots, which is a characteristic of species of *Rhizophora* (Cheng et al. 2015).

The combination of thickened exodermis and extensive and well-developed aerenchyma can make the species of this genus able to guarantee the necessary oxygen supply to the submerged roots, simultaneously creating an aerobic rhizosphere which favors Fe fixation in sediments. Also, the efficient mechanism of salt exclusion present in this species strongly restricts the entry of metals such as Fe, Zn and Cu and consequently decreases concentrations

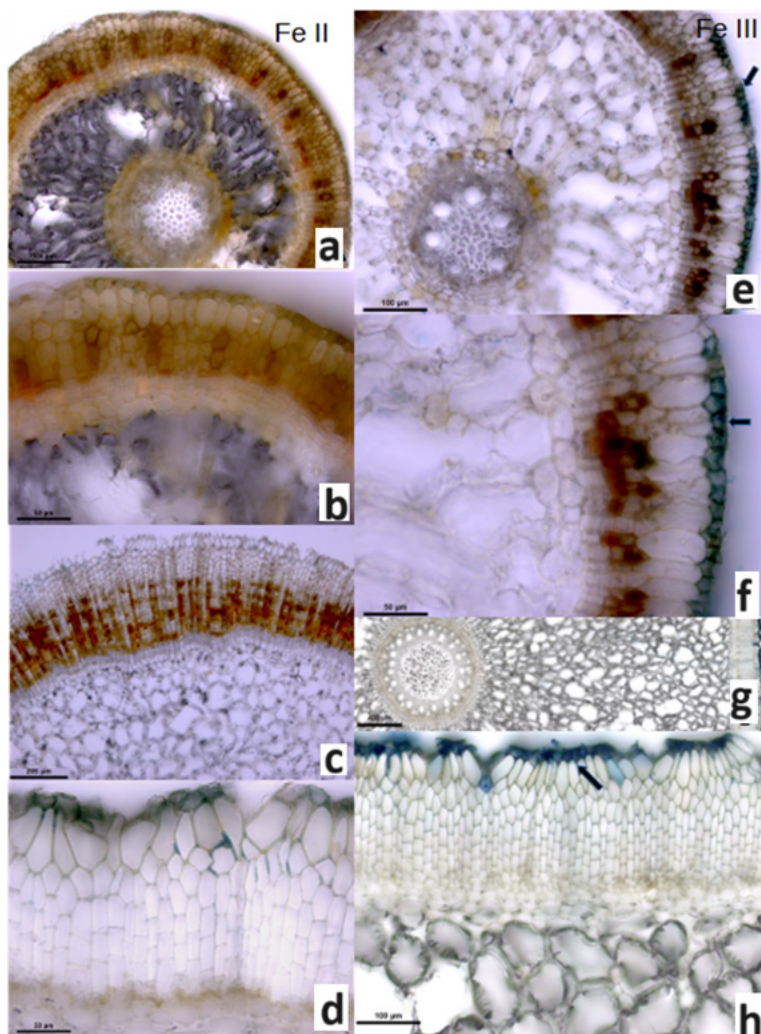


Figure 7. Iron histochemistry in cross-sections of roots of *R. mangle* a-h. a-b: Lillie's reagent test for Fe²⁺ (Fe II) in thin roots. c-d: Fe²⁺ in thin and thick roots (strand no significant accumulation). E-H Perl reagent for Fe³⁺ (Fe III). e-f: positive reaction on epidermis cells of the thin roots. g-h: Fe³⁺ positive reaction thickened roots in external periclinal cell walls of the outermost layer of suber. Blue coloration indicates positive reaction to the test (arrows).

of metals in their leaf tissues (Bernini et al. 2006). These characteristics have suggested *R. mangle* in studies of phytoremediation of coastal areas contaminated by metals (Colmer et al. 2003, Pi et al. 2011).

The detection of Fe^{3+} in other sections of the same roots was predominantly in the epidermis. Few point reactions were observed inside the other root tissues. Figure 7e presents an overview of a cross-section of the root, and a second cross-section with greater magnification of the image, detailing the positive reaction to the test in the outer periclinal cell walls of the epidermis (Figure 7f-h).

Leaves of *R. mangle* presented intense positive reactions to Fe^{2+} (Figure 8a-c), but little or no positive reaction to the presence of Fe^{3+} inside the cells (Figure 8d-e). This iron species is practically present throughout all leaf tissues, in the vicinity of both the adaxial and abaxial faces of the leaves and inside the conducting vessels.

Figure 8a shows the presence of Fe^{2+} the midrib leaf included in xylem and phloem. The presence of dissolved Fe in these cells is further proof of the translocation capacity of this metal between tissues. The release of iron in the xylem vessels necessitates the efflux of Fe from symplastic to apoplastic transport. Iron is usually present forming Fe^{3+} -citrate complexes

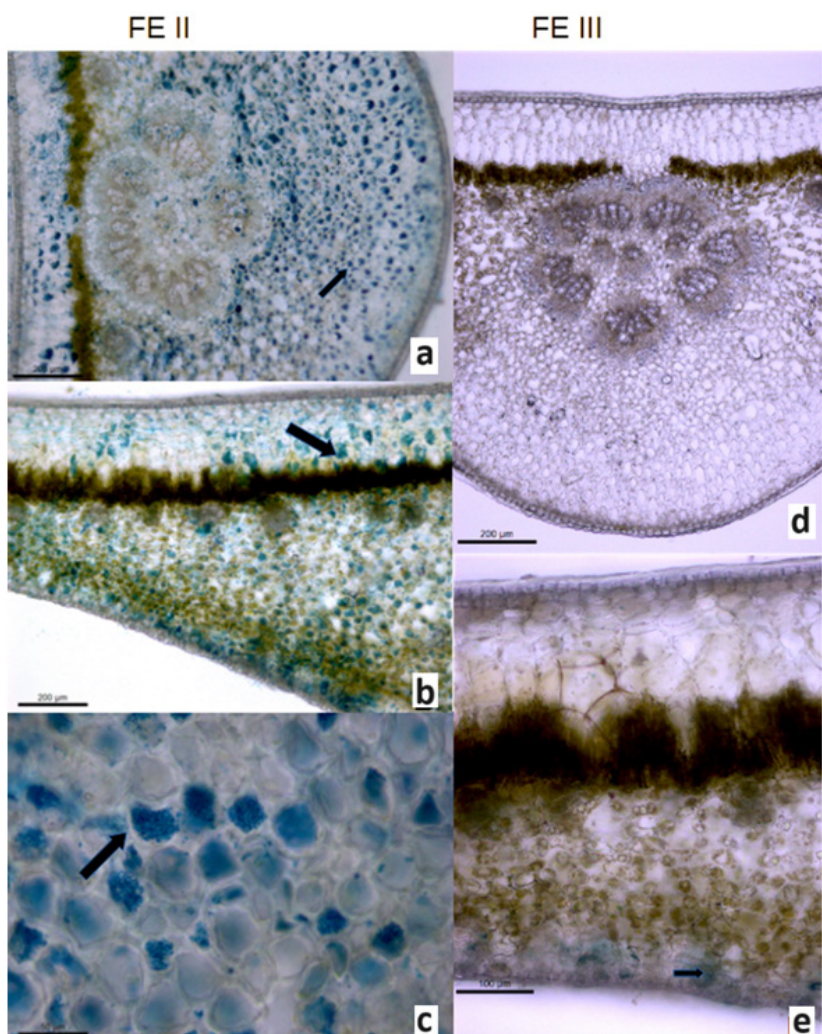


Figure 8. Fe^{2+} (FE II) and Fe^{3+} (FE III) histochemistry in cross-sections of leaves *R. mangle*. a-e. a-c: Lillie's reagent test showing accumulation of Fe^{2+} leaves of *Rhizophora mangle*. d-e: Perl reagent for Fe^{3+} in midrib and mesophyll leaves respectively.

in the xylem. However, the mechanism involved in iron absorption in xylem vessels and leaf tissues is still unclear (Kim & Guerinot 2007). Notwithstanding the presence of Fe in almost all leaf tissues, the bulk concentrations of Fe in leaves of *Rhizophora* were significantly lower than in leaves of *Avicennia*.

Figure 8b shows the Fe^{2+} also in the cross-section of *Rhizophora* leaves, focusing on the mesophyll area, where positive stains are also observed, indicating the presence of dissolved Fe in epidermis, hypodermis and the spongy parenchyma cells. Basically, Fe^{2+} was present in all leaf tissues in this species. However, no precipitation of iron was observed inside the leaves. (Figures 8c-d).

Previous studies (Cheng et al. 2010, 2015, 2020, Li et al. 2016, Arrivabene et al. 2016) have demonstrated the potential for decreased translocation of some metals from the roots to the aerial parts of plants due to the presence of iron plaques. However, in the present study it was observed that even in the presence of thick iron plaques, median concentrations of Fe^{2+} were translocated to the leaves of both species. The presence of precipitated Fe^{3+} in the epidermis of the roots from both *Avicennia* and *Rhizophora*, comprises another demonstration that in the Jaguaribe mangrove there is the formation of iron plaques, requiring more detailed studies considering other variables also important for their formation and functioning. In this study, histochemical tests indicated the presence of iron within the leaf structures, corroborating the analytical quantification of Fe levels mentioned above. The presence of iron, confirmed by the two analyses, demonstrates that the Jaguaribe mangrove, like other mangroves worldwide, absorbs metals from the sediments and at least part of the absorbed content is transported between the different tissues until reaching the leaves.

CONCLUSION

The results obtained in the present study on iron and copper distribution in these semiarid mangrove sediments and plants support earlier studies, obtained in humid mangroves, on the role of iron plaques in controlling metal uptake by mangrove trees. However, the actual impact of iron plaques in mediating metal uptake is, for the first time, simultaneously confirmed by a detailed microscopic analysis of Fe distribution in roots and leaf tissues. The results demonstrate that the iron plaques present in the mangrove roots act as a sink for Fe and possibly also for Cu, as verified by their preferential distribution in the external areas of the roots, particularly in the precipitated and less labile form, and contribute to a significant fraction of these metals contents in mangrove sediments.

On the other hand, the very low concentrations, below the detection limit, of Cu in interstitial waters and the absence of histochemical data for this element, prevent a more in-depth discussion of the role of iron plaques in the plant-soil dynamics of Cu and its distribution in plant tissues.

The histochemical analysis of Fe performed on the roots and leaves of both species, however, proved to be an effective methodology in the identification of the presence of Fe in plant tissues, and can be used in future studies. This analysis confirms the difference verified in Fe translocation comparing salt secreting species (*A. schaueriana*) with filtering species (*R. mangle*). Our results also showed, for the first time, the actual presence of metals in the salt excreting glands of *A. schaueriana* proper.

The sampling did not allow more robust conclusions about the behavior of iron plaques in relation to the biogeochemistry of metals of the Jaguaribe mangrove as a whole, making it necessary to develop more comprehensive

studies in relation to spatiality, and particularly in conducting future studies considering the role of seasonality in the formation and/or functioning of iron plaques.

Acknowledgments

The authors thank the help provided in field and laboratory work by the staff of the Coastal Biogeochemistry Laboratory, LABOMAR-UFC, in particular Isabelle Bezelga Caracas, Jorge Felipe Rocha and Leonardo Alem. This work was supported by the INCT-TMCOcean - Conselho Nacional de Desenvolvimento Científico e Tecnológico - CNPq grant number 405.765/2022-3 and Fundação Cearense de Apoio ao Desenvolvimento Científico e Tecnológico - FUNCAP grant number 00159-001-0009/2019-1.

REFERENCES

- ABOU SEEDO K, ABIDO MS, SALIH AA & ABAHUSSAIN A. 2007. Assessing heavy metals accumulation in the leaves and sediments of urban mangroves (*Avicennia marina* (Forsk.) Vierh.) in Bahrain. *Inter J Ecol* 2017: 3978216. <https://doi.org/10.1155/2017/3978216>.
- ALONGI DM, WATTAYAKORN G, BOYLE S, TIRENDI F, PAYN C & DIXON P. 2004. Influence of roots and climate on mineral and trace element storage and flux in tropical mangrove soils. *Biogeochem* 69: 105-123. <https://doi.org/10.1023/B:BIOG.0000031043.06245.af>.
- ARAÚJO JMDCA, FERREIRA TO, SUAREZ-ABELENDIA M, NÓBREGA GN, ALBUQUERQUE AGBM, CARVALHO BEZERRA A & OTERO XL. 2016. The role of bioturbation by *Ucides cordatus* crab in the fractionation and bioavailability of trace metals in tropical semiarid mangroves. *Mar Pollut Bull* 111: 194-202. <https://doi.org/10.1016/j.marpolbul.2016.07.011>.
- ARRIVABENE HP, CAMPOS CQ, SOUZA IC, WUNDERLIN DA, MILANEZ CRD & MACHADO SR. 2016. Differential bioaccumulation and translocation patterns in three mangrove plants experimentally exposed to iron. Consequences for environmental sensing. *Environ Pollut* 215: 302-313. <https://doi.org/10.1016/j.envpol.2016.05.019>.
- ARRIVABENE HP, SOUZA IC, CÔ WLO, CONTI MM, WUNDERLIN DA & MILANEZ CRD. 2015. Effect of pollution by particulate iron on the morphoanatomy, histochemistry, and bioaccumulation of three mangrove plant species in Brazil. *Chemosphere* 127: 27-34. <https://doi.org/10.1016/j.chemosphere.2015.01.011>.
- BANCROFT JD & GAMBLE M. 2008. *Theory and Practice of Histological Techniques*. 6th Edition, Churchill Livingstone: Elsevier, China. [https://www.scirp.org/\(S\(vtj3fa45qm1ean45vvffcz55\)\)/reference/ReferencesPapers.aspx?ReferenceID=1582193](https://www.scirp.org/(S(vtj3fa45qm1ean45vvffcz55))/reference/ReferencesPapers.aspx?ReferenceID=1582193).
- BATTY LC, BAKER AJM, WHEELER BD & CURTIS CD. 2000. The effect of pH and plaque on the uptake of Cu and Mn in *Phragmites australis* (Cav.) Trin ex. Steudel. *Ann Bot* 86: 647-653. <https://doi.org/10.1006/anbo.2000.1191>.
- BERNINI E, SILVA MAB, CARMO TMS & CUZZUOL GRF. 2006. Composição química do sedimento e de folhas das espécies do manguezal do estuário do Rio São Mateus, Espírito Santo, Brasil. *Rev Brasil Bot* 29: 689-699. <https://doi.org/10.1590/S0100-84042006000400018>.
- CHAKRABORTY P, RAMTEKE D & CHAKRABORTY S. 2015. Geochemical partitioning of Cu and Ni in mangrove sediments: relationships with their bioavailability. *Mar Pollut Bull* 93: 194-201. <https://doi.org/10.1016/j.marpolbul.2015.01.016>.
- CHAUDHURI P, NATH B & BIRCH G. 2014. Accumulation of trace metals in grey mangrove *Avicennia marina* fine nutritive roots: the role of rhizosphere processes. *Mar Pollut Bull* 79: 284-292. <https://doi.org/10.1016/j.marpolbul.2013.11.024>.
- CHENG H, LIU Y, TAM NFY, WANG X, LI SY, CHEN GZ & YE ZH. 2010. The role of radial oxygen loss and root anatomy on zinc uptake and tolerance in mangrove seedlings. *Environ Pollut* 158: 1189-1196. <https://doi.org/10.1016/j.envpol.2010.01.025>.
- CHENG H, WANG YS, FEI J, JIANG ZY & YE ZH. 2015. Differences in root aeration, iron plaque formation and waterlogging tolerance in six mangroves along a continuous tidal gradient. *Ecotoxicology* 24: 1659-1667. <https://doi.org/10.1007/s10646-015-1474-0>.
- CHENG HW, YOU-SHAO L, CHANG-DA Y, ZHI-HONG M, SHAFI W, MEI-LIN S & FUN-LIN Y. 2020. Mixture of Pb, Zn and Cu on root permeability and radial oxygen loss in the mangrove *Bruguiera gymnorrhiza*. *Ecotoxicology* 29: 691-697. <https://doi.org/10.1007/s10646-020-02234-z>.
- COLMER TD. 2003. Long-distance transport of gases in plants: A perspective on internal aeration and radial oxygen loss from roots. *Plant Cell Environ* 26: 17-36. <https://doi.org/10.1046/j.1365-3040.2003.00846.x>.
- CUZZUOL GRF & FIELDS A. 2001. Aspectos nutricionais na vegetação de manguezal do estuário do Rio Mucuri, Bahia, Brasil. *Rev Brasil Bot* 24: 227-234. <https://doi.org/10.1590/S0100-84042001000200013>.

- DEBORDE J, MARCHAND C, MOLNAR N, DELLA P & TARIK ML. 2015. Concentrations and fractionation of carbon, iron, sulfur, nitrogen and phosphorus in mangrove sediments along an intertidal gradient (semi-arid climate, New Caledonia). *J Mar Sci Engineer* 3: 52-72. <https://doi.org/10.3390/jmse3010052>.
- DI TOPPI LS, VURRO V, DE BENEDICTIS M, FALASCA G, ZANELLA L, MUSETTI R, LENUCCI MS, DALESSANDRO G & ALTAMURA MM. 2012. A biphasic response to cadmium stress in carrot: early acclimatory mechanisms give way to root collapse further to prolonged metal exposure. *Plant Physiol Biochem* 58: 269-279. <https://doi.org/10.1016/j.plaphy.2012.07.002>.
- DIAS FJS, CASTRO BM & LACERDA LD. 2018. Tidal and low-frequency currents off the Jaguaribe River estuary (4°S, 37°4'W), northeastern Brazil. *Ocean Dynamics* 68: 967-985. <https://doi.org/10.1007/s10236-018-1172-6>.
- FUNCEME. 2022. Portal Hidrológico do Ceará. Fundação Cearense de Meteorologia. Fortaleza, Assessed on 21st November 2022. <http://www.hidro.ce.gov.br/>.
- HOLLOWAY CJ, SANTOS IR, TAIT DR, SANDERS CJ, ROSE AL, SCHNETGER B, BRUMSACK HJ, MACKLIN PA, SIPPO JZ & MAHER DT. 2016. Manganese and iron release from mangrove porewaters: a significant component of oceanic budgets? *Mar Chem* 184: 43-52. <https://doi.org/10.1016/j.marchem.2016.05.013>.
- HOWARD J, HOYT S, ISENSEE K, PIDGEON E & TELSZEWSKI M. 2014. Coastal Blue Carbon: Methods for assessing carbon stocks and emissions factors in mangroves, tidal salt marshes, and seagrass meadows. Conservation International, Intergovernmental Oceanographic Commission of UNESCO, International Union for Conservation of Nature. Arlington, Virginia, USA. <https://www.cifor.org/knowledge/publication/5095/>.
- HUZY, ZHUYG, LIM, ZHANG LG, CAO ZH & SMITH FA. 2007. Sulphur (S)-induced enhancement of iron plaque formation in the rhizosphere reduces arsenic accumulation in rice (*Oriza sativa* L.) seedlings. *Environ Pollut* 147: 387-393. <https://doi.org/10.1016/j.envpol.2006.06.014>.
- INQUE T, NOHARA S, TAKAGI H & ANZAI Y. 2011. Contrast of nitrogen contents around roots of mangrove plants. *Plant Soil* 339: 471-483. <https://doi.org/10.1007/s11104-010-0604-y>.
- JIMENEZ JA, MAIA LP, SERRA J & MORAIS JO. 1999. Aeolian dune migration along the Ceará coast, north-eastern Brazil. *Sedimentology* 46: 689-701. <http://dx.doi.org/10.1046/j.1365-3091.1999.00240.x>.
- KIM SA & GUERINOT ML. 2007. Mining iron: Iron uptake and transport in plants. *FEBS Letters* 581: 2273-2280. <https://doi.org/10.1016/j.febslet.2007.04.043>.
- KRISTENSEN E, VALDEMARSEN T, MORAES PC, GÜTH AZ, SUMIDA PYG & QUINTANA CO. 2023. Anaerobic carbon oxidation in sediment of two Brazilian mangrove forests: the influence of tree roots and crab burrows. *Ocean Coas Res* 71: e23003. <https://doi.org/10.1590/2675-2824071.22040ek>.
- KUMAR A & RAMANATHAN A. 2015. Speciation of selected trace metals (Fe, Mn, Cu and Zn) with depth in the sediments of Sundarban mangroves: India and Bangladesh. *J Soils Sediments* 15: 2476-2486. <https://doi.org/10.1007/s11368-015-1257-5>.
- LACERDA LD, CARVALHO CEV, TANIZAKI KF, OVALLE ARC & REZENDE CE. 1993. The biogeochemistry and trace metals distribution of mangrove rhizospheres. *Biotropica* 25: 252-257. <https://doi.org/10.2307/2388783>.
- LACERDA LD, FERREIRA AC, WARD R & BORGES R. 2022. Mangrove trace-metal biogeochemistry response to global climate change. *Front Forest Globl Chan* 5, <https://doi.org/10.3389/ffgc.2022.817992>.
- LACERDA LD, SANTOS JA & MADRID RM. 2006. Copper emission factors from intensive shrimp aquaculture. *Mar Pollut Bull* 12: 1823-1826. <https://doi.org/10.1016/j.marpolbul.2006.09.012>.
- LEWIS M, PRYOR R & WILKING L. 2011. Fate and effects of anthropogenic chemicals in mangrove ecosystems: a review. *Environ Pollut* 159: 2328-2346. <https://doi.org/10.1016/j.envpol.2011.04.027>.
- LI R, CHAI M & QIU GY. 2016. Distribution, fraction, and ecological assessment of heavy metals in sediment-plant system in mangrove forest, South China Sea. *PLoS ONE* 11(1): e0147308.
- LIU JC, YAN CL, KATE LS, ZHANG RF & LU ZH. 2010. The distribution of acid-volatile sulfide and simultaneously extracted metals in sediments from a mangrove forest and adjacent mudflat in Zhangjiang Estuary, China. *Mar Pollut Bull* 60: 1209-1216. <https://doi.org/10.1016/j.marpolbul.2010.03.029>.
- MACFARLANE GR & BURCHETT MD. 2000. Cellular distribution of copper, lead and zinc in the grey mangrove, *Avicennia marina* (Forsk.) Vierh. *Aquat Bot* 68: 45-59. [https://doi.org/10.1016/S0304-3770\(00\)00105-4](https://doi.org/10.1016/S0304-3770(00)00105-4).
- MACFARLANE GR & BURCHETT MD. 2002. Toxicity, growth and accumulation relationships of copper, lead and zinc in the grey mangrove *Avicennia marina* (Forsk.) Vierh. *Mar Environ Res* 54: 65-84. [https://doi.org/10.1016/S0141-1136\(02\)00095-8](https://doi.org/10.1016/S0141-1136(02)00095-8).

- MACFARLANE GR, KOLLER CE & BLOMBERG SP. 2007. Accumulation and partitioning of heavy metals in mangroves: a synthesis of field-based studies. *Chemosphere* 69: 1454-1464.
- MACFARLANE GR, PULKOWNIK A & BURCHETT MD. 2003. Accumulation and distribution of heavy metals in the grey mangrove, *Avicennia marina* (Forsk.) Vierh. : biological indication potentiel. *Environ Pollut* 123: 139-151. [https://doi.org/10.1016/S0269-7491\(02\)00342-1](https://doi.org/10.1016/S0269-7491(02)00342-1).
- MACHADO W, GUEIROS BB, LISBOA-FILHO SD & LACERDA LD. 2005. Trace metals in mangrove seedlings: role of iron plaque formation. *Wetlands Ecol Manage* 13: 199-206. <https://doi.org/10.1016/j.chemosphere.2007.04.059>.
- MADI APLM, BOEGER MRT & REISSMANN CB. 2015. Distribution of Cu, Fe, Mn, and Zn in two mangroves of Southern Brazil. *Braz Arch Bio Technol* 58: 970-976. <https://doi.org/10.1590/S1516-89132015060255>.
- MARCHAND C, ALLENBACH M & LALLIER-VERGÈS E. 2011. Relationships between heavy metals distribution and organic matter cycling in mangrove sediments (Conception Bay, New Caledonia). *Geoderma* 160: 444-456. <https://doi.org/10.1016/j.geoderma.2010.10.015>.
- MARCHAND C, LALLIER-VERGÈS E, BLATZER F, ALBÉRIC P, COSSA D & BAILIF P. 2006. Heavy metals distribution in mangrove sediments along the mobile coastline of French Guiana. *Mar Chem* 98: 1-17. <https://doi.org/10.1016/j.marchem.2005.06.001>.
- MARINS RV, LACERDA LD, ARAÚJO ICS, FONSECA LV & SILVA FATF. 2020. Phosphorus and suspended matter retention in mangroves affected by shrimp farm effluents in NE Brazil. *An Acad Brasil Cienc* 92: e20200758. <https://doi.org/10.1590/0001-3765202020200758>.
- MARINS RV, LACERDA LD, GONÇALVES GO & PAIVA EC. 1997. Effects of root metabolism on the post-depositional mobilization of mercury in salt marsh soils. *Bull Environ Cont Toxicol* 58: 733-738. <https://doi.org/10.1007/s001289900394>.
- NAIDOO G, TISHA H & NAIDOO Y. 2014. Ecophysiological responses of the mangrove *Avicennia marina* to trace metal contamination. *Flora-Morphology, Distribution. Funct Ecol Plants* 209: 63-72. <https://doi.org/10.1016/j.flora.2013.10.003>.
- NATH B, BIRCH G & CHAUDHURI P. 2013. Trace metal biogeochemistry in mangrove ecosystems: a comparative assessment of acidified (by acid sulfate soils) and non-acidified sites. *Sci Tot Environ* 463: 667-674. <https://doi.org/10.1016/j.scitotenv.2013.06.024>.
- ONG CHE RG. 1999. Concentration of 7 heavy metals in sediments and mangrove root samples from Mai Po, Hong Kong. *Mar Pollut Bull* 39: 269-279. [https://doi.org/10.1016/S0025-326X\(99\)00056-9](https://doi.org/10.1016/S0025-326X(99)00056-9).
- OTERO XL, FERREIRA TO, VIDAL-TORRADO P & MACÍAS F. 2006. Spatial variation in pore water geochemistry in a mangrove system (Pai Matos island, Cananeia-Brazil). *Appl Geochem* 21: 2171-2186. <https://doi.org/10.1016/j.apgeochem.2006.07.012>.
- PI NA, TAM NFY & WONG MH. 2011. Formation of iron plaque on mangrove roots receiving wastewater and its role in immobilization of wastewater-borne pollutants. *Mar Pollut Bull* 63: 402-411. <https://doi.org/10.1016/j.marpolbul.2011.05.036>.
- PURNOBASUKI H & SUZUKI M. 2005. Functional anatomy of air conducting network on the pneumatophores of a mangrove plant, *Avicennia marina* (Forsk.) Vierh. *Asian J Plant Sci* 4: 334-347. <https://doi.org/10.3923/ajps.2005.334.347>.
- SCHOLANDER PF. 1968. How mangroves desalinate seawater. *Physiol Plantarum* 21: 251-261. <https://doi.org/10.1111/j.1399-3054.1968.tb00724.x>.
- SOUZA IS, ARAUJO GS, CRUZ ACF, FONSECA TG, CAMARGO JBDA, MEDEIROS GF & ABESSA DMS. 2015. Changes in bioaccumulation and translocation patterns between root and leaves of *Avicennia schaueriana* as adaptive response to different levels of metals in mangrove system. *Mar Pollut Bull* 94: 176-184. <https://doi.org/10.1016/j.marpolbul.2015.02.032>.
- SOUZA IS, ARAUJO GS, CRUZ ACF, FONSECA TG, CAMARGO JBDA, MEDEIROS GF & ABESSA DMS. 2016. Using an integrated approach to assess the sediment quality of an estuary from the semi-arid coast of Brazil. *Mar Pollut Bull* 104: 70-82. <https://doi.org/10.1016/j.marpolbul.2016.02.009>.
- SOUZA IS, MOROZESKY M, DUARTE ID, BONOMO MM, ROCHA D, FURLAN LM, ARRIVABENE HP, MONFERRÁ MV, WUNDERLIN DA & MILANEZ CRD. 2014. Matching pollution with adaptive changes in mangrove plants by multivariate statistics. A case study, *Rhizophora mangle* from four neotropical mangroves in Brazil. *Chemosphere* 108: 115-124. <https://doi.org/10.1016/j.chemosphere.2014.02.066>.
- SRUTHI P, SHACKIRA AM & PUTHUR JT. 2017. Heavy metal detoxification mechanisms in halophytes: an overview. *Wetlands Ecol Manage* 25: 129-148. <https://doi.org/10.1007/s11273-016-9513-z>.
- TAYLOR GJ & CROWDER AA. 1983. Use of the DCB technique for extraction of hydrous iron oxides from roots of

wetland plants. *Amer J Bot* 70: 1254-1257. <https://doi.org/10.2307/2443295>.

TOMLINSON PB. 1986. *The Botany of Mangroves*. Cambridge: Cambridge University Press, UK, 678 p.

TRIPATHI RD, TRIPATHI P, DWIVEDI S, KUMAR A, MISHRA A, CHAUHAN PS, NORTON GJ & NAUTIYAL CS. 2014. Roles for root iron plaque in sequestration and uptake of heavy metals and metalloids in aquatic and wetland plants. *Metallomics* 6: 1789-1800. <https://doi.org/10.1039/c4mt00111g>.

VIOLLIER E, INGLETT PW, HUNTER K, ROYCHOUDHURY AN & VAN CAPPELLEN P. 2000. The ferrozine method revisited: Fe (II)/Fe (III) determination in natural waters. *Appl Geochem* 15: 785-790. [https://doi.org/10.1016/S0883-2927\(99\)00097-9](https://doi.org/10.1016/S0883-2927(99)00097-9).

XU B & YU S. 2013. Root iron plaque formation and characteristics under N₂ flushing and its effects on translocation of Zn and Cd in paddy rice seedlings (*Oryza sativa*). *An Bot* 111: 1189-1195. <https://doi.org/10.1093/aob/mct072>.

YEOMANS JC & BREMNER JM. 1988. A rapid and precise method for routine determination of organic carbon in soil. *Comm Soil Sci Plant Anal* 19: 1467-1476. <https://doi.org/10.1080/00103628809368027>.

SUPPLEMENTARY MATERIAL

Figure S1.

How to cite

LACERDA LD, CAVALCANTE IBK, SOARES AA & MARINS RV. 2024. Mobility, bioavailability and distribution of Fe and Cu in mangroves (*Avicennia schaueriana* and *Rhizophora mangle*) from a semiarid coast in NE Brazil. *An Acad Bras Cienc* 96: e20231075. DOI: 10.1590/0001-3765202420231075.

Manuscript received on September 26, 2023; accepted for publication on March 4, 2024

LUIZ D. LACERDA¹

<https://orcid.org/0000-0002-3496-0785>

INGRA B.K. CAVALCANTE²

<https://orcid.org/0000-0002-1060-1948>

ARLETE A. SOARES²

<https://orcid.org/0000-0002-0329-0619>

ROZANE V. MARINS¹

<https://orcid.org/0000-0002-3744-4006>

¹Universidade Federal do Ceará, Instituto de Ciências do Mar, Avenida Abolição, 3207, 60165-081 Fortaleza, CE, Brazil

²Universidade Federal do Ceará, Departamento de Biologia, Campus do Pici, Bloco 948, 60440-900 Fortaleza, CE, Brazil

Correspondence to: **Luiz D. Lacerda**

E-mail: ldrude1956@gmail.com

Author contributions

LD Lacerda, designed the study, sampling and analysis, writing and reviewing, funding. IKC Cavalcante, sampling and analysis, writing. AA Soares, microscopy analysis, writing, reviewing. RV Marins, designed the study, sampling and analysis, writing.

